Curcumin Ameliorates Neuroinflammation, Neurodegeneration, and Memory Deficits in p25 Transgenic Mouse Model that Bears Hallmarks of Alzheimer's Disease

Jeyapriya Raja Sundaram[a,b,1], **Charlene Priscilla Poore**[a,c], **Noor Hazim Bin Sulaimee**[a,b], **Tej Pareek**[e], **Wei Fun Cheong**[a,c], **Markus R. Wenk**[a,c], **Harish C. Pant**[f], **Sally A. Frautschy**[g,h], **Chian-Ming Low**[a,b,d], **Sashi Kesavapany**[a,c,*]

[a]Neurobiology and Ageing Program, Centre for Life Sciences, Yong Loo Lin School of Medicine, National University of Singapore, Singapore

[b]Department of Pharmacology, Yong Loo Lin School of Medicine, National University of Singapore, Singapore

[c]Department of Biochemistry, Yong Loo Lin School of Medicine, National University of Singapore, Singapore

[d]Department of Anaesthesia, Yong Loo Lin School of Medicine, National University of Singapore, Singapore

[e]Department of Pediatrics, Case Western Reserve University, Cleveland, OH, USA

[f]National Institute of Neurological Disorders and Stroke, National Institutes of Health, Bethesda, MD, USA

[g]Department of Neurology, University of California, Los Angeles, CA, USA

[h]Geriatric Research Education and Clinical Center, Veterans Greater Los Angeles Healthcare System, Los Angeles, CA, USA

Abstract

Several studies have indicated that neuroinflammation is indeed associated with neurodegenerative disease pathology. However, failures of recent clinical trials of anti-inflammatory agents in neurodegenerative disorders have emphasized the need to better understand the complexity of the neuroinflammatory process in order to unravel its link with neurodegeneration. Deregulation of Cyclin-dependent kinase 5 (Cdk5) activity by production of its hyperactivator p25 is involved in the formation of tau and amyloid pathology reminiscent of Alzheimer's disease (AD). Recent studies show an association between p25/Cdk5 hyperactivation and robust neuroinflammation. In addition, we recently reported the novel link between the p25/Cdk5 hyperactivation-induced

[*]Correspondence to: Sashi Kesavapany, NTU Institute for Health Technologies, Nanyang Technological University, Research Techno Plaza, XFrontiers Block, #02-07, 50 Nanyang Drive, Singapore 637553. Tel.: +65 65923516; Fax: +65 67943 735; SashiKesavapany@ntu.edu.sg.
[1]Current address: Duke-NUS Medical School Singapore, Singapore.

inflammatory responses and neurodegenerative changes using a transgenic mouse that overexpresses p25 (p25Tg). In this study, we aimed to understand the effects of early intervention with a potent natural anti-inflammatory agent, curcumin, on p25-mediated neuroinflammation and the progression of neurodegeneration in p25Tg mice. The results from this study showed that curcumin effectively counteracted the p25-mediated glial activation and pro-inflammatory chemokines/cytokines production in p25Tg mice. Moreover, this curcumin-mediated suppression of neuroinflammation reduced the progression of p25-induced tau/amyloid pathology and in turn ameliorated the p25-induced cognitive impairments. It is widely acknowledged that to treat AD, one must target the early-stage of pathological changes to protect neurons from irreversible damage. In line with this, our results demonstrated that early intervention of inflammation could reduce the progression of AD-like pathological outcomes. Moreover, our data provide a rationale for the potential use of curcuminoids in the treatment of inflammation associated neurodegenerative diseases.

Keywords

Amyloid; Cdk5; curcumin; neurodegeneration; neuroinflammation; p25; tau

INTRODUCTION

Cyclin-dependent kinase 5 (Cdk5), a member of the Cdk family of serine/threonine kinases, plays important roles in regulating development and maintenance of the central nervous system (CNS) [1, 2]. The cleavage of the Cdk5 activator p35 by calpain releases a C-terminal p25 fragment, which deregulates and hyperactivates Cdk5 activity [3-5]. Substantial evidence now support a model in which p25-mediated Cdk5 deregulation is involved in the regulation of many signaling pathways that are closely linked with the pathological development of various neurodegenerative diseases including Alzheimer's disease (AD) [6-9]. Characterization of the inducible p25 transgenic (Tg) mice further supports the contribution of p25/Cdk5 hyperactivation in the development of neuropathological changes including neurofibrillary pathology, abnormal amyloid-β protein precursor (AβPP) processing and cognitive dysfunction [10-13]. Evidence from studies in other transgenic AD mouse models indicated that accumulation of amyloid peptide starts intraneuronally and this is one of the earliest events in the AD pathogenesis progression [14-19]. Similarly, intraneuronal amyloid accumulations become apparent from 8 weeks of induction of p25 expression in p25Tg mice [20]. Although these p25 mice, like other AD mice models, do not completely replicate all aspects of the disease, they develop specific pathological features which closely mimic aspects of human AD and they can be useful in understanding some of the mechanisms involved in the progression of AD.

Studies have shown that neuroinflammation is associated with the development of various neurodegenerative diseases [21-23]. Prominent reactive gliosis and chemokine production were observed very early at one week of induction of p25 expression in p25Tg mice. Recently, astrogliosis and its persistent activation has been identified as one of the primary causative factor to AD development [24,25]. However, the complexity of this association is still not fully elucidated. Our previous study gave further support to this concept where we

reported a novel molecular mechanism of early neuroinflammatory changes and its importance in triggering the neurodegeneration using p25 overexpressing transgenic mice [20]. In the present study, we extended our investigation on p25/Cdk5-mediated neuroinflammation to determine the effect of early intervention of pro-inflammatory changes on the progression of neurodegeneration in p25Tg mice using curcumin, a potent anti-inflammatory agent.

Curcumin is a natural dietary supplement that can cross the blood-brain barrier in its native form and is active against sustained neuroinflammation without any serious adverse effects [26, 27]. Curcumin, the main component of the Indian spice turmeric, is well known for its antioxidant, anti-amyloidogenic, anti-inflammatory, and anti-oncogenic properties [28-31]. However, the major limitation in the use of curcumin is its low bioavailability due to its low solubility in water and poor oral adsorption [32]. Over the years, a number of strategies have been used to increase the bioavailability of curcumin and some of them have been successful. A research group led by Sally Frautschy at UCLA formulated a novel curcumin with solid lipid curcumin particle (SLCP) preparation, called "Longvida". Chronic administration of SLCP-curcumin (4 months, 500–2000 ppm) to an AD mouse model (APPsw Tg2576) significantly increases the free or the unconjugated form of curcumin in plasma (0.095–0.465 μM) as well as in brain (1.276–1.428 μM) [33]. A subsequent *in vivo* study in tau transgenic mice with SLCP-curcumin specified that 500 ppm curcumin treatment resulted in significant free curcumin levels (198.3 nM ± 5.9) in the brain [34]. Furthermore, SLCP curcumin administration (650 mg) in healthy volunteers caused substantial levels of free curcumin in plasma compared to the 95% curcuminoid extracts. This enriched bioavailability of SLCP curcumin could be either due to increased absorption or due to reduced conversion of free curcumin to conjugated products [33, 35, 36]. The smaller particle size of SLCP curcumin and its specialized coating (made up of specific ratio of phospholipids and free fatty acids) enables it to be directly transported to the lymphatic system. Hence it is less exposed to the metabolic enzymes and the majority remains as the free form of curcumin [37]. A recent *in vitro* study further confirmed the increased solubility of SLCP curcumin compared with unmodified curcumin [38].

In this study, p25Tg mice were fed with Longvida-curcumin in supplemented feed pellets during the induction of p25 expression. We found that curcumin treatment inhibited the major events of p25-mediated neuroinflammation in p25Tg mice. In particular, curcumin efficiently reduced p25 overexpression-induced astrocyte activation and pro-inflammatory chemokines/cytokines release. Moreover, this curcumin-mediated inhibition of neuroinflammation blocked the progression of p25-induced neurodegenerative changes including tau and amyloid accumulations and rescued neurocognitive impairments in p25Tg mice. Our experimental evidence collectively indicated that early inhibition of inflammatory triggers could prevent the progression of neurodegenerative changes. Our study evaluated the potential relevance of Longvida-curcumin as a tool to prevent the progression of neuroinflammation and subsequent neurodegeneration.

METHODS

p25 transgenic mouse model

p25 single transgenic mice (C57BL/6-Tg (tetO-CDK5R1/GFP) 337Lht/J, The Jackson Laboratory, Stock No: 005706) were crossed with CaMKIIα single transgenic mice (B6; CBA-Tg (Camk2a-tTA) 1Mmay/DboJ, The Jackson Laboratory, Stock No: 007004) to generate bi-transgenic offspring (p25Tg mice) that inducibly overexpress the human p25 gene under the control of the CaMKIIα promoter-regulated tet-off system. p25Tg mice were maintained on doxycycline (Sigma; 200 μg/ml, in drinking water) from conception until 6 weeks postnatal to avoid any possible developmental consequences from the p25 expression. Hemizygous mice of either sex were used in all the experiments. Wild-type littermates were used as control groups.

All experiments with animals were carried out according to protocols approved by the Institutional Animal Care & Use Committee (IACUC) of the National University of Singapore.

Curcumin treatment in p25Tg mice

p25 expression was induced in 6-week-old mice by removal of doxycycline in water and concurrently treated with an optimized curcumin formulation, Longvida (prepared using the SLCP technology, Verdure Sciences), orally via their feed (4 g/kg (0.8 g curcumin/kg) of chow prepared by Harlan Teklad) for 12 weeks.

Antibodies

Antibodies used for both immunohistochemistry and Western blot analyses were mouse and rabbit anti-GFAP (Sigma, 1 : 1,000), mouse monoclonal anti-Cd11b (Millipore, 1 : 200), mouse monoclonal anti-cPLA2 (Santa Cruz Biotechnology, 1 : 200), mouse monoclonal anti-PHF-tau (clones AT8, Pierce, 1 : 100), mouse monoclonal anti-beta-amyloid 1–42 (Millipore, 1 : 100), rabbit anti-cleaved caspase-3 (Cell Signaling Technology, 1 : 200), rabbit polyclonal anti-Cdk5 (C8, 1 : 500, Santa Cruz Biotechnology), mouse monoclonal anti-GFP (Roche, 1 : 500), and mouse anti-α-tubulin (Sigma, 1 : 10,000) antibodies. Secondary horseradish peroxidase-conjugated antibodies (GE Healthcare, 1 : 1000) were used for Western blot analyses and secondary fluorescence-conjugated antibodies Alexa Fluor 488 and Alexa Fluor 594 (Invitrogen, 1 : 200) were used for immunohistochemistry.

Histochemical studies

12-week induced (18-week-old) p25Tg/control mice (with and without curcumin treatment, $n = 3$ for each group) were anesthetized with mixtures of ketamine (75 mg/kg) and medepomidin (1 mg/kg) and transcardially perfused with freshly made 4% paraformaldehyde (PFA/PBS). Immunofluorescence staining was performed with 16 μm thick cryo-brain sections according to our published protocol [20]. Thioflavin staining was carried out as described earlier [13, 39]. Confocal images were taken at 40X magnification. Bielschowsky silver staining were performed according to a published protocol [40]. Silver staining images were taken at 20X magnification.

Western blot analyses

Brain lysates from 12-week induced (18-week-old) p25Tg/control mice (with and without curcumin treatment, $n = 3$ for each group) were prepared as described [41]. Mice brain lysates were resolved on 4–20% polyacrylamide gels, blotted onto nitrocellulose membranes and then immunoprobed as described previously [20].

In vitro kinase assays

Cdk5 activity levels in brain lysates from 12-week induced (18-week-old) p25Tg/control mice (with and without curcumin treatment) were measured using kinase assays as described previously [42].

Real-Time PCR

Quantification of chemokines/cytokines expression levels were performed using real-time PCR (RT-PCR) with RNA samples extracted from 12-week induced (18-week-old) p25Tg/control mice brains (with and without curcumin treatment) according to our previously published protocol [20].

Cytosolic phospholipase A2 (cPLA2) activity assay

cPLA2 activity levels were determined for the brain lysates from 12-week induced p25Tg/control mice (with and without curcumin treatment) using cPLA2 activity assay kit (Cayman Chemical). The results were normalized against total protein concentration (BCA assays, Pierce Biotechnology).

Lipid analyses using high-performance liquid chromatography/mass spectrometry

Total lipids were extracted from brain samples of 12-week induced (18-week-old) p25Tg/control mice (with and without curcumin treatment) as described previously [20, 43]. Separation and quantification of lysophosphatidylcholine (LPC) levels from total lipids were performed according to our published protocol [20].

Behavioral studies

The radial arm maze study was carried out using the 8-arm radial maze as per our earlier published protocol [13]. Reference memory errors (entering a non-baited arm) and working memory errors (number of re-entry into baited arms) were calculated and analyzed for 12-week induced (18-week-old) p25Tg/control mice groups (with and without curcumin treatment).

Statistical analyses

Data are expressed as the mean of at least three values ± standard error mean (s.e.m). Statistical significance was determined using one-way ANOVA followed by *post-hoc* Tukey's test and repeated measures ANOVA followed by *post-hoc* Tukey's test (Radial Maze analyses). *p*-value for statistical significance was defined as $p < 0.05$.

RESULTS

Curcumin suppresses p25-induced astrocyte activation in p25Tg mice

The control and p25Tg mice groups were fed with curcumin-enriched feed for 12 weeks during the induction of p25 expression. Curcumin-treated control mice appeared healthy with well-groomed coats and normal exploratory behaviors. Firstly, equivalent levels of p25 expression were confirmed in the curcumin-treated as well as non-treated p25Tg mice groups using immunohistochemistry (Fig. 1A) and Western blot analyses (Fig. 1B) with anti-GFP (Green fluorescent protein) antibody. To further investigate whether curcumin has a regulatory role on p25/Cdk5 hyperactivation, kinase assays and immunoblot analyses were performed and results indicated that there was no obvious change in Cdk5 protein levels between the 12-week induced curcumin-treated and non-treated p25Tg mice groups (Fig. 1C, D). However, p25-mediated Cdk5 hyperactivity was decreased in curcumin treated 12-week induced p25Tg mice compared to the non-treated p25Tg mice (Fig. 1E).

We then analyzed astrocyte activation levels in curcumin treated and non-treated control/ p25Tg mice brain samples using immunohistochemistry with anti-GFAP (Glial fibrillary acidic protein) antibody. Results revealed that the intensity of GFAP staining was remarkably reduced in the cortex as well as in the hippocampus of 12-week induced curcumin-treated p25Tg mice compared to non-treated p25Tg mice group (Fig. 2A). Furthermore, Western blot analyses of GFAP levels confirmed that there was an approximate 2-3-fold reduction in GFAP expression in the forebrain of curcumin-treated p25Tg mice compared to non-treated p25Tg mice (Fig. 2B, C). To explore further the anti-inflammatory effect of curcumin in p25Tg mice, we examined the cPLA2 expression as well as LPC production levels in curcumin treated and non-treated p25Tg mice. Western blot quantification and cPLA2 activity assay results showed an approximately 3-fold reduction in p25-mediated cPLA2 upregulation in 12-week induced curcumin-treated p25Tg mice (Fig. 2D-F). Furthermore, mass spectrometry data demonstrated that LPC levels were markedly decreased by curcumin treatment in p25Tg mice (Fig. 2G).

Curcumin antagonizes p25-mediated pro-inflammatory cascade in p25Tg mice

We next investigated the curcumin effects on microglial activation levels in p25Tg mice brains using immunohistochemical studies and Western blot analyses. Altered immunostaining patterns with anti-Cd11b, a microglial activation marker was observed in both cortical and hippocampal regions of curcumin-treated 12-week induced p25Tg mice brains compared to those in the non-treated p25Tg mice (Fig. 3A). Further examination using western blot analyses revealed that there was a modest reduction in microglial activation in curcumin-treated 12-week induced p25Tg mice (Fig. 3B, C) and these results demonstrated that the total activation of microglia was not completely inhibited by curcumin in p25Tg mice. We then performed RT-PCR analyses to assess the chemokine/cytokine expression levels in curcumin-treated and non-treated p25Tg/control mice in order to investigate whether curcumin has any role on p25-mediated pro-inflammatory responses. The predominantly anti-inflammatory cytokine TGF-β (transforming growth factor-β) levels were unaltered in curcumin treated p25Tg mice. However, the pro-inflammatory cytokines MIP-1α (macrophage inflammatory protein-1α), TNF-α (tumor necrosis factor-alpha), and

IL-1β (Interleukin-1α) expression levels in p25Tg mice were significantly downregulated by curcumin treatment (Fig. 3D-G). These results collectively concluded that the pro-inflammatory state was blocked by curcumin in p25Tg mice.

Curcumin attenuates p25-mediated neuropathology in p25Tg mice

Hyperphosphorylation of tau and amyloid accumulations are conspicuous events in p25-mediated neurodegeneration [10, 11, 20]. To gain insight into the role of curcumin on p25-induced neurodegeneration, we first studied the tau hyperphosphorylation levels using immunohistochemistry and Western blot analyses. AT8 immunostaining levels were reduced prominently in curcumin-treated p25Tg mice compared to non-treated (Fig. 4A). This finding is consistent with the Western blot results, in which approximately a 2-fold reduction in AT8 expression levels were observed in curcumin-treated p25Tg mice (Fig. 4B, C).

We next investigated the impact of curcumin treatment on p25-induced amyloid accumulations in the cortex and hippocampus of the mice brain using immunofluorescence, thioflavin and Bielschowsky silver staining analyses. The results showed a remarkable reduction in $A\beta_{1-42}$ immunostaining in curcumin-treated p25Tg mice compared to non-treated mice (Fig. 5A). Moreover, thioflavin and silver staining results were identical to the immunohistochemistry findings (Fig. 5B, C). Overall, the results supported the conclusion that curcumin robustly prevented the progression of p25-induced tau hyperphosphorylation and amyloid aggregations in p25Tg mice.

Curcumin protects neurons against p25-mediated apoptosis and ameliorates neurocognitive deficits in p25Tg mice

Apparent forebrain atrophy and neuronal apoptosis are seen in p25Tg mice brain after 8–12 weeks induction of p25 expression [10, 12, 13]. In the present study, we investigated whether curcumin confers neuroprotection against p25-induced neuronal death. Immunohistochemical analyses results showed that cleaved caspase-3 immunostaining was reduced in 12-week induced p25Tg mice after curcumin treatment (Fig. 6A).

We next examined whether this neuroprotective effect of curcumin treatment is able to rescue the p25 overexpression-stimulated neurocognitive deficits in p25Tg mice. Spatial memory tasks were performed using radial arm maze analyses and curcumin-treated p25Tg mice displayed better performance compared to non-treated p25Tg mice. Working memory errors were reduced almost back to the normal levels (Fig. 6B) and reference memory errors decreased in curcumin-treated p25Tg mice (Fig. 6C). Based on these results, we concluded that curcumin has a neuroprotective capability to restore p25-induced cognitive deficits in p25Tg mice.

DISCUSSION

Our group previously reported that robust astrocyte activation and subsequent neuroinflammation were prominent features in p25Tg mice brain. In addition, our previous *in vitro* findings indicated that the inhibition of early neuroinflammation by reducing LPC and cPLA2 signaling reversed the progression of p25-mediated neuropathology [20]. In this study, we focused on the detailed understanding of the effects of inhibiting p25/Cdk5

hyperactivation-mediated inflammatory triggers on the progression of the neurodegeneration *in vivo* in p25Tg mice using curcumin, a potent anti-inflammatory agent.

An obvious reduction in astrocyte activation in curcumin treated p25Tg mice was the first prominent finding in this study. In addition, curcumin-mediated reduction in astrocyte activation was previously reported in various *in vitro* and *in vivo* neurodegenerative disease model studies [44-47]. However, the principal underlying mechanism(s) responsible for efficacy in AD models remains still unclear. In our previous report, we determined that cPLA2 activation and LPC release were crucial events behind p25-induced astrocyte activation [20]. Moreover, the results in this study specified that curcumin mediated downregulation of cPLA2/LPC signaling pathways in p25Tg mice might be responsible for the reduction of glial activation, particularly astrocytes. Furthermore, our results using parent curcumin and its metabolites (bisdemethoxycurcumin, curcumin glucuronide, curcumin sulphate, and tetrahydrocurcumin) on human glioblastoma cells (A172) activated with LPC clearly demonstrated that parent curcumin (free form) was more active in reducing the glial activation compared to its other metabolites (Supplementary Figure 1).

Our group and others previously reported that p25Tg mice displayed increased accumulation of hyperphosphorylated tau and intraneuronal amyloid deposits in the forebrain [10, 11, 20]. Evidence from studies in other transgenic AD mouse models indicate that accumulation of amyloid peptide starts intraneuronally and these intraneuronal amyloid-β (Aβ) accumulations are one of the earliest events and also key players in the AD pathogenesis progression [14-19]. In this study, the striking observation of remarkable clearance of p25-induced amyloid accumulations and reduced tau hyperphosphorylation in curcumin treated p25 mice strongly supported the hypothesis that early inhibition of neuroinflammation can slow down the development of later pathological events. Our results are also consistent with previous studies using other AD mice models showing that curcumin reduces tau hyperphosphorylation [48]. Numerous studies have suggested that curcumin is a potent anti-amyloidogenic agent that inhibits Aβ aggregation, conferring protection against Aβ-induced cell death [28, 45, 49-51]. In addition, studies reported that curcumin cleared amyloid aggregates via the induction of phagocytosis by microglia [52-56]. However, the actual mechanism behind this reduction has not been fully elucidated. It is widely reported that curcumin acts on several pathways and so, its effects may not be due to just a single pathway effect. Firstly, the anti-inflammatory effect of curcumin might attenuate the inflammation induced tau hyperphosphorylation and Aβ aggregation. Secondly, the negative regulatory role of curcumin on Cdk5 hyperactivation observed in p25Tg mice suggesting a possible direct inhibitory effect of curcumin on tau hyperphosphorylation via modulating the activity of a prominent tau kinase. Although, it has already been reported that curcumin inhibits GSK-3β (glycogen synthase kinase-3 beta) [57], there has not been any prior evidence concerning curcumin-mediated inhibition of Cdk5 hyperactivity. Therefore, further investigation on curcumin-mediated specific reduction in Cdk5 hyperactivity would pave the way to the development of an alternative targeting strategy against aberrantly hyperactivated Cdk5 in neurodegenerative diseases.

It has been reported that the phagocytic ability of microglia may be dampened by the expression of pro-inflammatory cytokines especially TNF-α [58]. In addition, it has

previously been demonstrated that TGF-β expression might promote the microglial-mediated clearance of Aβ [59]. In the present study, our observations of selective downregulation of TNF-α expression levels without altering the level of TGF-β by curcumin treatment in p25Tg mice suggest that curcumin may trigger a change in glial phenotype to promote the phagocytic ability of microglia to clear amyloid aggregates. However, further validation of this observation is needed to fully understand the role of curcumin on microglial activation. Results from this study also showed that p25-mediated neuronal apoptosis and spatial memory deficits were reduced after curcumin treatment in p25Tg mice. We believe that curcumin-mediated reductions in the p25-mediated pathologies including aberrant astrocyte activation, upregulated pro-inflammatory cytokines especially TNF-α, and intraneuronal tau/amyloid accumulations could be the reasons behind this curcumin-mediated reversal of neuronal apoptosis and cognitive deficits. In another recent *in vivo* study, we characterized a tetra transgenic mouse model that overexpresses both CIP (Cdk5 inhibitor peptide, a specific inhibitor for p25/Cdk5 hyperactivation) [60, 61] and p25 in the forebrain and we observed a remarkable reduction in hyperphosphorylated tau, amyloid accumulations, and brain atrophy. However, neuroinflammation was not completely reversed in these mice [13]. Therefore, it would be interesting to investigate whether curcumin can be additive to this protection in addition to the CIP effect to bring about a complete reversal of p25-mediated neurotoxicity. Furthermore, we believe that this combinational therapy could be an improved therapeutic approach to treat neurodegenerative diseases with multiple pathologies such as AD. The development of such curcumin therapeutics such as Longvida-curcumin also opens avenues to investigate how to increase the bioavailability of curcumin further and explore alternative delivery systems.

Our data in this report with Longvida-curcumin supported our hypothesis that early inhibition of neuroinflammation can reduce the development of later pathological events associated with tau and amyloid pathologies, reduce neuronal death and improve cognitive function. A key future experiment would be to treat these mice after these pathological hallmarks are evident to see if curcumin can reverse these effects which will determine whether curcumin will be a prophylactic or therapeutic compound.

Supplementary Material

Refer to Web version on PubMed Central for supplementary material.

ACKNOWLEDGMENTS

REFERENCES

[1]. Nikolic M, Chou MM, Lu W, Mayer BJ, Tsai LH (1998) The p35/Cdk5 kinase is a neuron-specific Rac effector that inhibits Pak1 activity. Nature 395, 194–198. [PubMed: 9744280]

[2]. Smith DS, Greer PL, Tsai LH (2001) Cdk5 on the brain. Cell Growth Differ 12, 277–283. [PubMed: 11432802]

[3]. Kusakawa G, Saito T, Onuki R, Ishiguro K, Kishimoto T, Hisanaga S (2000) Calpain-dependent proteolytic cleavage of the p35 cyclin-dependent kinase 5 activator to p25. J Biol Chem 275, 17166–17172. [PubMed: 10748088]

[4]. Lee MS, Kwon YT, Li M, Peng J, Friedlander RM, Tsai LH (2000) Neurotoxicity induces cleavage of p35 to p25 by calpain. Nature 405, 360–364. [PubMed: 10830966]

[5]. Patrick GN, Zukerberg L, Nikolic M, de la Monte S, Dikkes P, Tsai LH (1999) Conversion of p35 to p25 deregulates Cdk5 activity and promotes neurodegeneration. Nature 402, 615–622. [PubMed: 10604467]

[6]. Nguyen MD, Julien JP (2003) Cyclin-dependent kinase 5 in amyotrophic lateral sclerosis. Neurosignals 12, 215–220. [PubMed: 14673208]

[7]. Lau LF, Seymour PA, Sanner MA, Schachter JB (2002) Cdk5 as a drug target for the treatment of Alzheimer's disease. J Mol Neurosci 19, 267–273. [PubMed: 12540052]

[8]. Smith PD, Crocker SJ, Jackson-Lewis V, Jordan-Sciutto KL, Hayley S, Mount MP, O'Hare MJ, Callaghan S, Slack RS, Przedborski S, Anisman H, Park DS (2003) Cyclin-dependent kinase 5 is a mediator of dopaminergic neuron loss in a mouse model of Parkinson's disease. Proc Natl Acad Sci U S A 100, 13650–13655. [PubMed: 14595022]

[9]. Cruz JC, Tsai LH (2004) Cdk5 deregulation in the pathogenesis of Alzheimer's disease. Trends Mol Med 10, 452–458. [PubMed: 15350898]

[10]. Cruz JC, Tseng HC, Goldman JA, Shih H, Tsai LH (2003) Aberrant Cdk5 activation by p25 triggers pathological events leading to neurodegeneration and neurofibrillary tangles. Neuron 40, 471–483. [PubMed: 14642273]

[11]. Cruz JC, Kim D, Moy LY, Dobbin MM, Sun X, Bronson RT, Tsai LH (2006) p25/cyclin-dependent kinase 5 induces production and intraneuronal accumulation of amyloid beta in vivo. J Neurosci 26, 10536–10541. [PubMed: 17035538]

[12]. Muyllaert D, Terwel D, Kremer A, Sennvik K, Borghgraef P, Devijver H, Dewachter I, Van Leuven F (2008) Neurodegeneration and neuroinflammation in cdk5/p25-inducible mice: A model for hippocampal sclerosis and neocortical degeneration. Am J Pathol 172, 470–485. [PubMed: 18202185]

[13]. Sundaram JR, Poore CP, Sulaimee NH, Pareek T, Asad AB, Rajkumar R, Cheong WF, Wenk MR, Dawe GS, Chuang KH, Pant HC, Kesavapany S (2013) Specific inhibition of p25/Cdk5 activity by the Cdk5 inhibitory peptide reduces neurodegeneration in vivo. J Neurosci 33, 334–343. [PubMed: 23283346]

[14]. Lord A, Kalimo H, Eckman C, Zhang XQ, Lannfelt L, Nilsson LN (2006) The Arctic Alzheimer mutation facilitates early intraneuronal Abeta aggregation and senile plaque formation in transgenic mice. Neurobiol Aging 27, 67–77. [PubMed: 16298242]

[15]. Oakley H, Cole SL, Logan S, Maus E, Shao P, Craft J, Guillozet-Bongaarts A, Ohno M, Disterhoft J, Van Eldik L, Berry R, Vassar R (2006) Intraneuronal beta-amyloid aggregates, neurodegeneration, and neuron loss in transgenic mice with five familial Alzheimer's disease mutations: Potential factors in amyloid plaque formation. J Neurosci 26, 10129–10140. [PubMed: 17021169]

[16]. Oddo S, Caccamo A, Shepherd JD, Murphy MP, Golde TE, Kayed R, Metherate R, Mattson MP, Akbari Y, LaFerla FM (2003) Triple-transgenic model of Alzheimer's disease with plaques and tangles: Intracellular Abeta and synaptic dysfunction. Neuron 39, 409–421. [PubMed: 12895417]

[17]. Shie FS, LeBoeuf RC, Jin LW (2003) Early intraneuronal Abeta deposition in the hippocampus of APP transgenic mice. Neuroreport 14, 123–129. [PubMed: 12544843]

[18]. Wirths O, Multhaup G, Czech C, Blanchard V, Moussaoui S, Tremp G, Pradier L, Beyreuther K, Bayer TA (2001) Intraneuronal Abeta accumulation precedes plaque formation in beta-amyloid precursor protein and presenilin-1 double-transgenic mice. Neurosci Lett 306, 116–120. [PubMed: 11403971]

[19]. Billings LM, Oddo S, Green KN, McGaugh JL, LaFerla FM (2005) Intraneuronal Abeta causes the onset of early Alzheimer's disease-related cognitive deficits in transgenic mice. Neuron 45, 675–688. [PubMed: 15748844]

[20]. Sundaram JR, Chan ES, Poore CP, Pareek TK, Cheong WF, Shui G, Tang N, Low CM, Wenk MR, Kesavapany S (2012) Cdk5/p25-induced cytosolic PLA2-mediated lysophosphatidylcholine

production regulates neuroinflammation and triggers neurodegeneration. J Neurosci 32, 1020–1034. [PubMed: 22262900]

[21]. Frank-Cannon TC, Alto LT, McAlpine FE, Tansey MG (2009) Does neuroinflammation fan the flame in neurodegenerative diseases? Mol Neurodegener 4, 47. [PubMed: 19917131]

[22]. Heneka MT, Kummer MP, Latz E (2014) Innate immune activation in neurodegenerative disease. Nat Rev Immunol 14, 463–477. [PubMed: 24962261]

[23]. Amor S, Puentes F, Baker D, van der Valk P (2010) Inflammation in neurodegenerative diseases. Immunology 129, 154–169. [PubMed: 20561356]

[24]. Jain P, Wadhwa PK, Jadhav HR (2015) Reactive astrogliosis: Role in Alzheimer's disease. CNS Neurol Disord Drug Targets 14, 872–879. [PubMed: 26166438]

[25]. Osborn LM, Kamphuis W, Wadman WJ, Hol EM (2016) Astrogliosis: An integral player in the pathogenesis of Alzheimer's disease. Prog Neurobiol 144, 121–141. [PubMed: 26797041]

[26]. Menon VP, Sudheer AR (2007) Antioxidant and anti-inflammatory properties of curcumin. Adv Exp Med Biol 595, 105–125. [PubMed: 17569207]

[27]. Ammon HP, Wahl MA (1991) Pharmacology of curcuma longa. Planta Med 57, 1–7. [PubMed: 2062949]

[28]. Garcia-Alloza M, Borrelli LA, Rozkalne A, Hyman BT, Bacskai BJ (2007) Curcumin labels amyloid pathology *in vivo*, disrupts existing plaques, and partially restores distorted neurites in an Alzheimer mouse model. J Neurochem 102, 1095–1104. [PubMed: 17472706]

[29]. Monroy A, Lithgow GJ, Alavez S (2013) Curcumin and neurodegenerative diseases. Biofactors 39, 122–132. [PubMed: 23303664]

[30]. Mishra S, Palanivelu K (2008) The effect of curcumin (turmeric) on Alzheimer's disease: An overview. Ann Indian Acad Neurol 11, 13–19. [PubMed: 19966973]

[31]. Prasad S, Aggarwal BB (2011) Turmeric, the golden spice: From traditional medicine to modern medicine. In Herbal Medicine: Biomolecular and Clinical Aspects, 2nd edition, Benzie IFF, Wachtel-Galor S, eds. CRC Press/Taylor & Francis, Boca Raton, FL.

[32]. Anand P, Kunnumakkara AB, Newman RA, Aggarwal BB (2007) Bioavailability of curcumin: Problems and promises. Mol Pharm 4, 807–818. [PubMed: 17999464]

[33]. Begum AN, Jones MR, Lim GP, Morihara T, Kim P, Heath DD, Rock CL, Pruitt MA, Yang F, Hudspeth B, Hu S, Faull KF, Teter B, Cole GM, Frautschy SA (2008) Curcumin structure-function, bioavailability, and efficacy in models of neuroinflammation and Alzheimer's disease. J Pharmacol Exp Ther 326, 196–208. [PubMed: 18417733]

[34]. Ma QL, Zuo X, Yang F, Ubeda OJ, Gant DJ, Alaverdyan M, Teng E, Hu S, Chen PP, Maiti P, Teter B, Cole GM, Frautschy SA (2013) Curcumin suppresses soluble tau dimers and corrects molecular chaperone, synaptic, and behavioral deficits in aged human tau transgenic mice. J Biol Chem 288, 4056–4065. [PubMed: 23264626]

[35]. Gota VS, Maru GB, Soni TG, Gandhi TR, Kochar N, Agarwal MG (2010) Safety and pharmacokinetics of a solid lipid curcumin particle formulation in osteosarcoma patients and healthy volunteers. J Agric Food Chem 58, 2095–2099. [PubMed: 20092313]

[36]. Dadhaniya P, Patel C, Muchhara J, Bhadja N, Mathuria N, Vachhani K, Soni MG (2011) Safety assessment of a solid lipid curcumin particle preparation: Acute and subchronic toxicity studies. Food Chem Toxicol 49, 1834–1842. [PubMed: 21571027]

[37]. Ghalandarlaki N, Alizadeh AM, Ashkani-Esfahani S (2014) Nanotechnology-applied curcumin for different diseases therapy. Biomed Res Int 2014, 394264. [PubMed: 24995293]

[38]. Nahar PP, Slitt AL, Seeram NP (2015) Anti-inflammatory effects of novel standardized solid lipid curcumin formulations. J Med Food 18, 786–792. [PubMed: 25490740]

[39]. Sun A, Nguyen XV, Bing G (2002) Comparative analysis of an improved thioflavin-s stain, Gallyas silver stain, and immunohistochemistry for neurofibrillary tangle demonstration on the same sections. J Histochem Cytochem 50, 463–472. [PubMed: 11897799]

[40]. Litchfield S, Nagy Z (2001) New temperature modification makes the Bielschowsky silver stain reproducible. Acta Neuropathol 101, 17–21. [PubMed: 11194935]

[41]. Kesavapany S, Li BS, Amin N, Zheng YL, Grant P, Pant HC (2004) Neuronal cyclin-dependent kinase 5: Role in nervous system function and its specific inhibition by the Cdk5 inhibitory peptide. Biochim Biophys Acta 1697, 143–153. [PubMed: 15023357]

[42]. Poore CP, Sundaram JR, Pareek TK, Fu A, Amin N, Mohamed NE, Zheng YL, Goh AX, Lai MK, Ip NY, Pant HC, Kesavapany S (2010) Cdk5-mediated phosphorylation of delta-catenin regulates its localization and GluR2-mediated synaptic activity. J Neurosci 30, 8457–8467. [PubMed: 20573893]

[43]. Bremer J, Norum KR (1982) Metabolism of very long-chain monounsaturated fatty acids (22:1) and the adaptation to their presence in the diet. J Lipid Res 23, 243–256. [PubMed: 7042878]

[44]. Wang HM, Zhao YX, Zhang S, Liu GD, Kang WY, Tang HD, Ding JQ, Chen SD (2010) PPARgamma agonist curcumin reduces the amyloid-beta-stimulated inflammatory responses in primary astrocytes. J Alzheimers Dis 20, 1189–1199. [PubMed: 20413894]

[45]. Lim GP, Chu T, Yang F, Beech W, Frautschy SA, Cole GM (2001) The curry spice curcumin reduces oxidative damage and amyloid pathology in an Alzheimer transgenic mouse. J Neurosci 21, 8370–8377. [PubMed: 11606625]

[46]. Tripanichkul W, Jaroensuppaperch EO (2013) Ameliorating effects of curcumin on 6-OHDA-induced dopaminergic denervation, glial response, and SOD1 reduction in the striatum of hemiparkinsonian mice. Eur Rev Med Pharmacol Sci 17, 1360–1368. [PubMed: 23740450]

[47]. Wang Y, Yin H, Wang L, Shuboy A, Lou J, Han B, Zhang X, Li J (2013) Curcumin as a potential treatment for Alzheimer's disease: A study of the effects of curcumin on hippocampal expression of glial fibrillary acidic protein. Am J Chin Med 41, 59–70. [PubMed: 23336507]

[48]. Shytle RD, Tan J, Bickford PC, Rezai-Zadeh K, Hou L, Zeng J, Sanberg PR, Sanberg CD, Alberte RS, Fink RC, Roschek B Jr (2012) Optimized turmeric extract reduces beta-Amyloid and phosphorylated Tau protein burden in Alzheimer's transgenic mice. Curr Alzheimer Res 9, 500–506. [PubMed: 21875408]

[49]. Zhang C, Browne A, Child D, Tanzi RE (2010) Curcumin decreases amyloid-beta peptide levels by attenuating the maturation of amyloid-beta precursor protein. J Biol Chem 285, 28472–28480. [PubMed: 20622013]

[50]. Yang F, Lim GP, Begum AN, Ubeda OJ, Simmons MR, Ambegaokar SS, Chen PP, Kayed R, Glabe CG, Frautschy SA, Cole GM (2005) Curcumin inhibits formation of amyloid beta oligomers and fibrils, binds plaques, and reduces amyloid in vivo. J Biol Chem 280, 5892–5901. [PubMed: 15590663]

[51]. Frautschy SA, Hu W, Kim P, Miller SA, Chu T, Harris-White ME, Cole GM (2001) Phenolic anti-inflammatory antioxidant reversal of Abeta-induced cognitive deficits and neuropathology. Neurobiol Aging 22, 993–1005. [PubMed: 11755008]

[52]. Gagliardi S, Ghirmai S, Abel KJ, Lanier M, Gardai SJ, Lee C, Cashman JR (2011) Evaluation in vitro of synthetic curcumins as agents promoting monocytic gene expression related to beta-amyloid clearance. Chem Res Toxicol 25, 101–112. [PubMed: 22029407]

[53]. Cashman JR, Gagliardi S, Lanier M, Ghirmai S, Abel KJ, Fiala M (2012) Curcumins promote monocytic gene expression related to beta-amyloid and superoxide dismutase clearance. Neurodegener Dis 10, 274–276. [PubMed: 22156608]

[54]. Cashman JR, Ghirmai S, Abel KJ, Fiala M (2008) Immune defects in Alzheimer's disease: New medications development. BMC Neurosci 9(Suppl 2), S13. [PubMed: 19090986]

[55]. Park SY, Jin ML, Kim YH, Kim Y, Lee SJ (2012) Anti-inflammatory effects of aromatic-turmerone through blocking of NF-kappaB, JNK, and p38 MAPK signaling pathways in amyloid beta-stimulated microglia. Int Immunopharmacol 14, 13–20. [PubMed: 22728094]

[56]. Kim HY, Park EJ, Joe EH, Jou I (2003) Curcumin suppresses Janus kinase-STAT inflammatory signaling through activation of Src homology 2 domain-containing tyrosine phosphatase 2 in brain microglia. J Immunol 171, 6072–6079. [PubMed: 14634121]

[57]. Huang HC, Xu K, Jiang ZF (2012) Curcumin-mediated neuroprotection against amyloid-beta-induced mitochondrial dysfunction involves the inhibition of GSK-3beta. J Alzheimers Dis 32, 981–996. [PubMed: 22886017]

[58]. Koenigsknecht-Talboo J, Landreth GE (2005) Microglial phagocytosis induced by fibrillar beta-amyloid and IgGs are differentially regulated by proinflammatory cytokines. J Neurosci 25, 8240–8249. [PubMed: 16148231]

[59]. Wyss-Coray T, Lin C, Yan F, Yu GQ, Rohde M, McConlogue L, Masliah E, Mucke L (2001) TGF-beta1 promotes microglial amyloid-beta clearance and reduces plaque burden in transgenic mice. Nat Med 7, 612–618. [PubMed: 11329064]

[60]. Shukla V, Zheng YL, Mishra SK, Amin ND, Steiner J, Grant P, Kesavapany S, Pant HC (2013) A truncated peptide from p35, a Cdk5 activator, prevents Alzheimer's disease phenotypes in model mice. FASEB J 27, 174–186. [PubMed: 23038754]

[61]. Shukla V, Seo J, Binukumar BK, Amin ND, Reddy P, Grant P, Kuntz S, Kesavapany S, Steiner J, Mishra SK, Tsai LH, Pant HC (2017) TFP5, a peptide inhibitor of aberrant and hyperactive Cdk5/p25, attenuates pathological phenotypes and restores synaptic function in CK-p25Tg mice. J Alzheimers Dis 56, 335–349. [PubMed: 28085018]
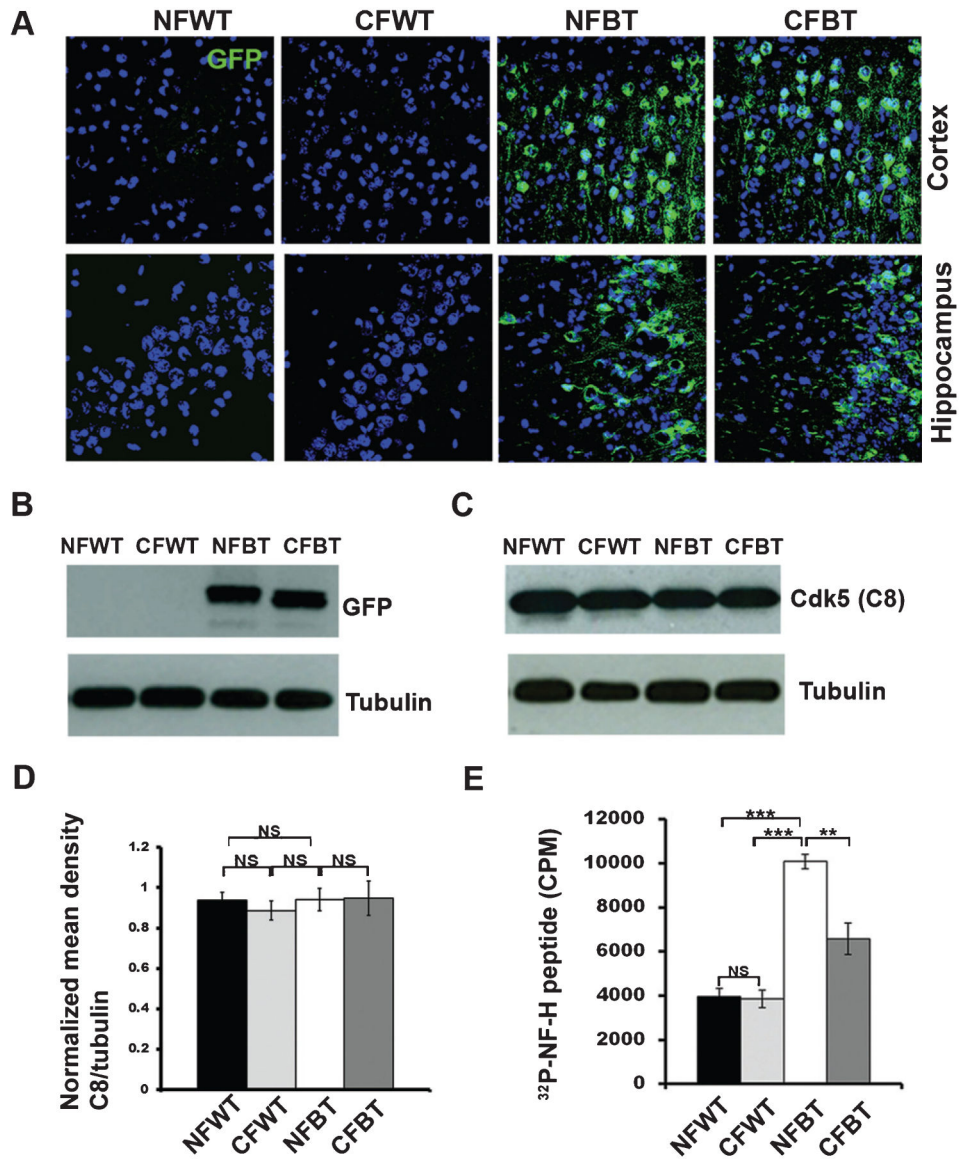
Fig. 1.
Expression and activity levels of Cdk5 in curcumin-treated p25Tg mice. A) Confocal images (from the cortex (layer 2/3) (top panels) and hippocampus (CA3 region) (bottom panels) of the brain sections and from 18-week-old wild type mice with normal feed (NFWT), wild type mice with curcumin feed (CFWT), 12-week induced (18-week-old) p25Tg mice with normal feed (NFBT), and p25Tg mice with curcumin feed (CFBT) using anti-GFP antibody ($n = 3$). Scale bars represent 20 μm. B) Immunoblot analyses results of brain lysates from the samples same as in (A) using anti-GFP antibody ($n = 3$). C) Western blot analyses results of brain lysates from 12-week induced p25Tg/control mice with/without curcumin treatment using anti-C8 antibodies ($n = 3$). D) Quantification of C8 immunoblots in C by densitometric scanning (NS $p > 0.05$). E) Kinase assay results of the brain lysates from the samples same as in A ($n = 3$) (***$p < 0.001$, **$p < 0.01$, and NS $p > 0.05$) (one-way ANOVA followed by *post-hoc* Tukey's test). Error bars indicate ± s.e.m.
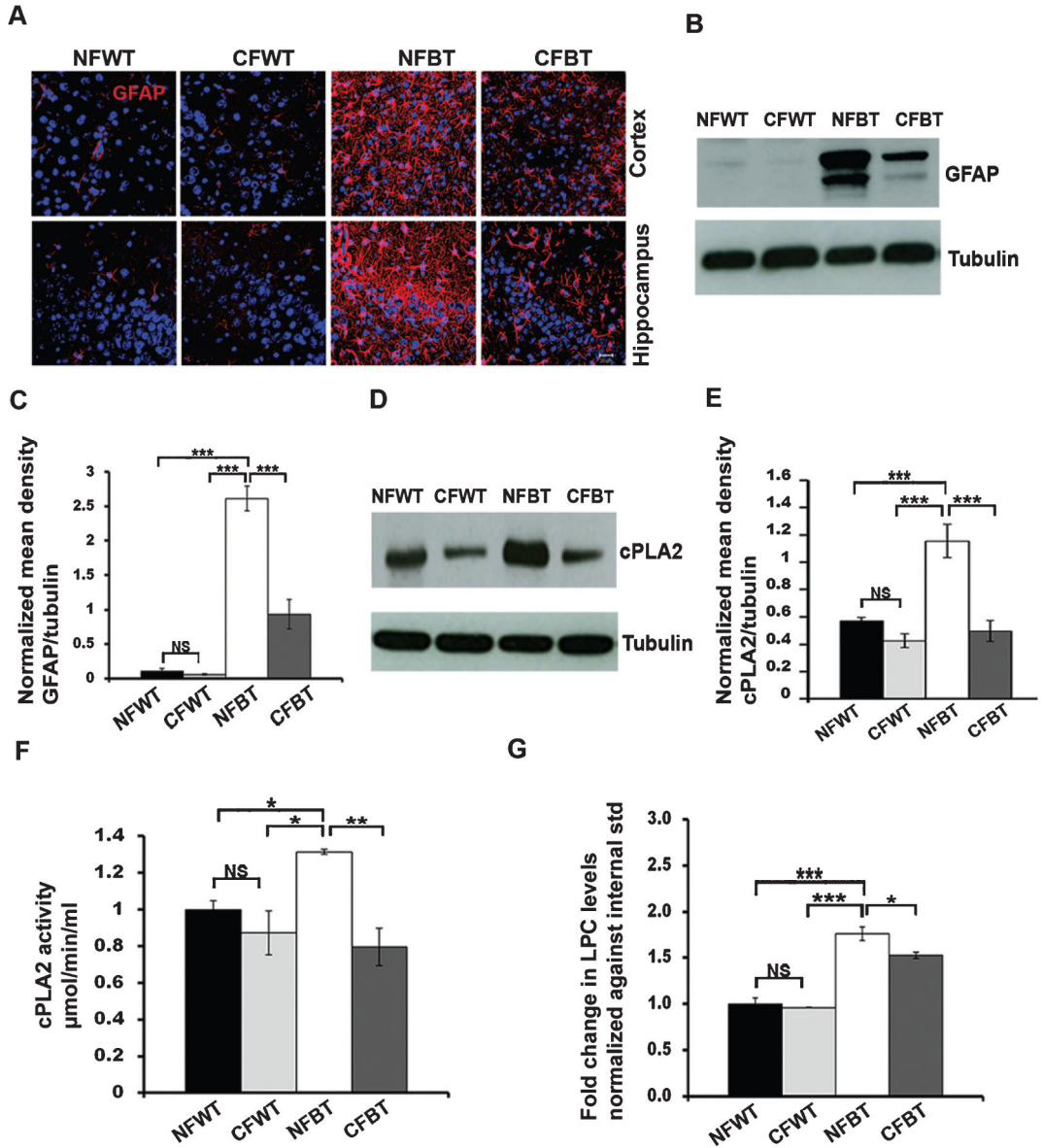
Fig. 2.
Curcumin reduces p25-induced astrocyte activation in p25Tg mice. A) Representative immunofluorescence images from the cortex (layer 2/3) (top panels) and hippocampus (CA3 region) (bottom panels) of the brain sections from 18-week-old wild type mice with normal feed (NFWT), wild type mice with curcumin feed (CFWT), 12-week induced (18-week old) p25Tg mice with normal feed (NFBT), and p25Tg mice with curcumin feed (CFBT) ($n = 3$) using anti-GFAP (red) and DAPI (blue). Scale bars represent 20 μm. B) Immunoblot analyses results of brain lysates from the samples same as in (A) using anti-GFAP antibody ($n = 3$). C) Quantification of GFAP immunoblots in by densitometric scanning (***$p < 0.001$, one-way ANOVA followed by *post-hoc* Tukey's test). D) Western blot analyses results of brain lysates from 18-week-old NFWT, CFWT, 12-week induced (18-week-old) NFBT, and CFBT mice ($n = 3$) using anti-cPLA2 and anti-tubulin (bottom panel) antibodies.

E) Quantification of immunoblots in (A) by densitometric scanning (***$p < 0.001$, **$p < 0.01$, *$p < 0.05$ and NS $p > 0.05$). F) cPLA2 activity assay results for the mice groups same as in (D) (**$p < 0.01$, *$p < 0.05$, and NS $p > 0.05$). G) Lysophosphatidylcholine (LPC) levels were analyzed using mass spectrometric analyses with lipids extracted from the forebrain samples of the mice groups same as in (A) ($n = 3$) (***$p < 0.001$, *$p < 0.05$, and NS $p > 0.05$) (one-way ANOVA followed by *post-hoc* Tukey's test). Error bars indicate ± s.e.m.
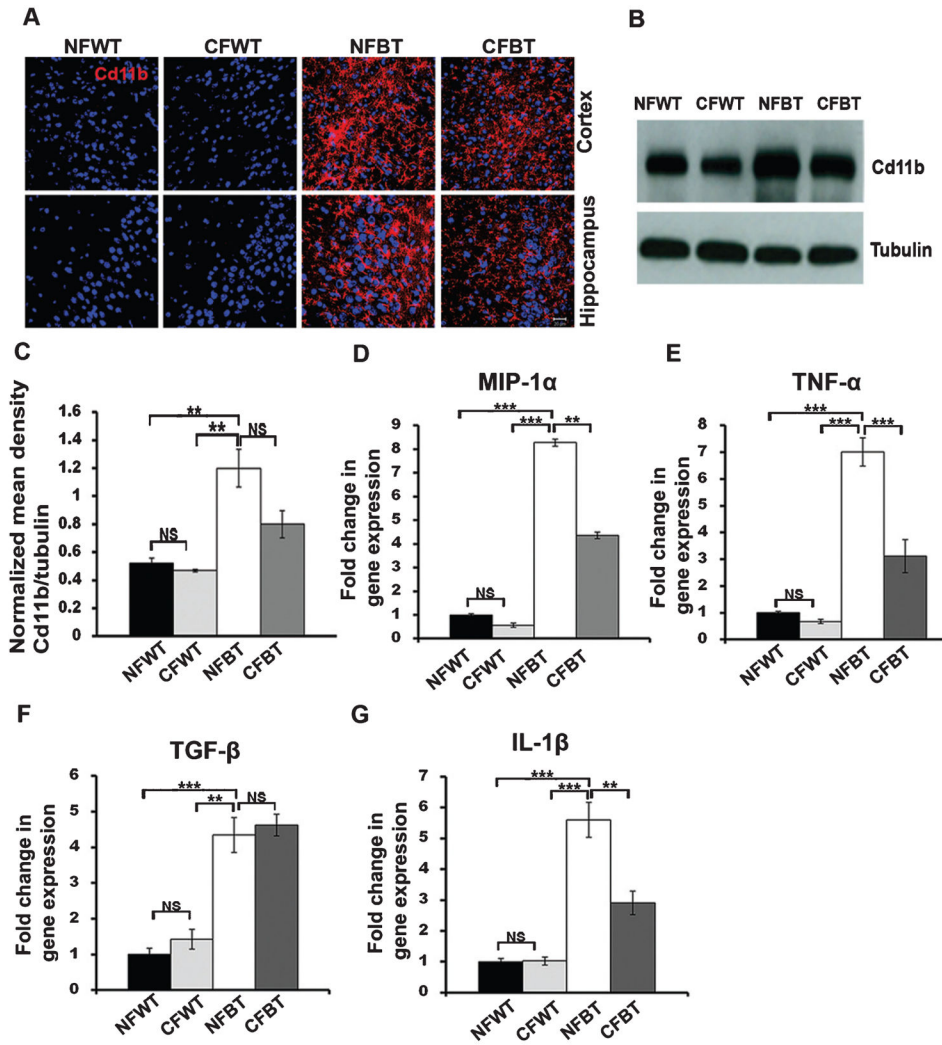
Fig. 3.

Reduced pro-inflammatory microglial activation and chemokine/cytokine expression levels in curcumin-treated p25Tg mice. A) Confocal images from the cortex and hippocampus of the brain sections from 18-week-old wild type mice with normal feed (NFWT), wild type mice with curcumin feed (CFWT), 12-week induced (18-week-old) p25Tg mice with normal feed (NFBT), and p25Tg mice with curcumin feed (CFBT) ($n = 3$) using anti-Cd11b antibody (red). Nuclei were stained with DAPI (blue). Scale bars represent 20 μm. B) Western blot analyses results of brain lysates from 12-week induced p25Tg/control mice with/without curcumin treatment using anti-Cd11b antibody ($n = 3$). C) Quantification of Cd11b immunoblots in (B) by densitometric scanning (**$p < 0.01$ and NS $p > 0.05$) (one-way ANOVA followed by *post-hoc* Tukey's test). Real-Time PCR results for (D) MIP-1α, (E) TNF-α, (F) TGF-β, and (G) IL-β expression levels in 12-week induced p25Tg/control mice with/without curcumin treatment ($n = 3$) (***$p < 0.001$, **$p < 0.01$, and NS $p > 0.05$) (one-way ANOVA followed by *post-hoc* Tukey's test). Error bars indicate ± s.e.m.
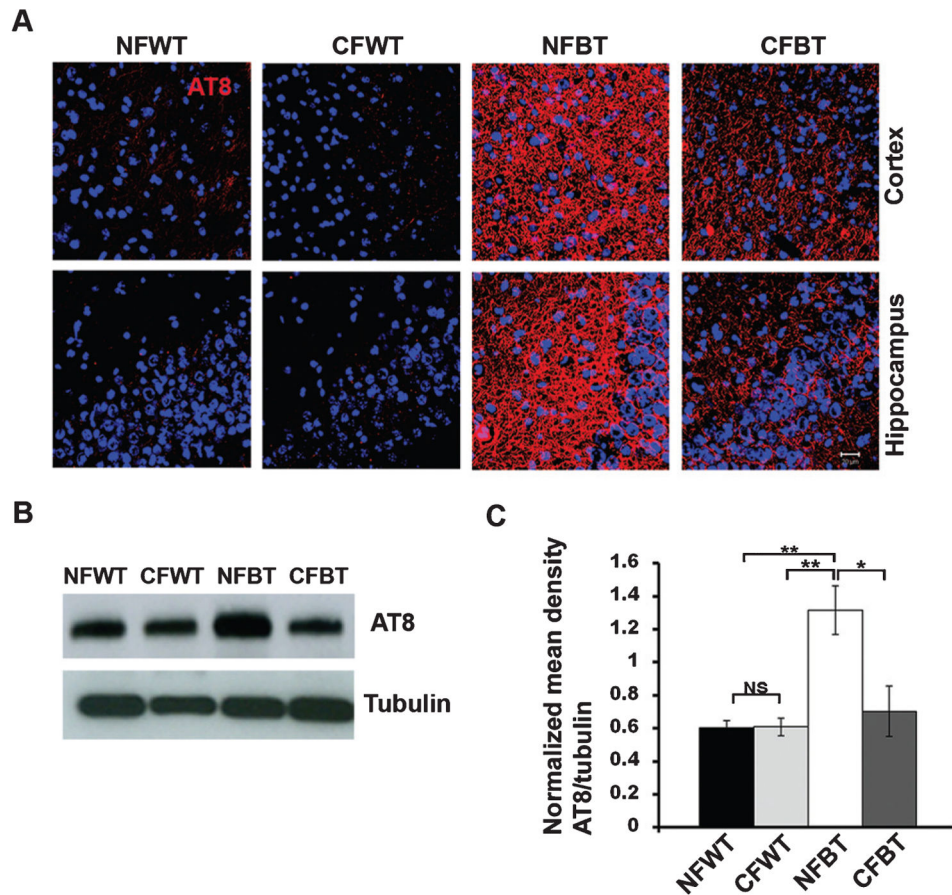
Fig. 4.
Curcumin attenuates p25-mediated tau hyperphosphorylation in p25Tg mice. A) Brain sections from 18-week-old wild type mice with normal feed (NFWT), wild type mice with curcumin feed (CFWT), 12-week induced (18-week-old) p25Tg mice with normal feed (NFBT), and p25Tg mice with curcumin feed (CFBT) ($n = 3$) were immunostained with phospho-tau antibody AT8 (red). Nuclei were stained with DAPI (blue). Scale bars represent 20 μm. B) Immunoblot analyses results of brain lysates from 12-week induced p25Tg/control mice with/without curcumin treatment using anti-AT8 antibody ($n = 3$). C) Quantification of immunoblots in (B) by densitometric scanning (**$p < 0.01$, *$p < 0.05$, and NS $p > 0.05$) (one-way ANOVA followed by *post-hoc* Tukey's test). Error bars indicate ± s.e.m.
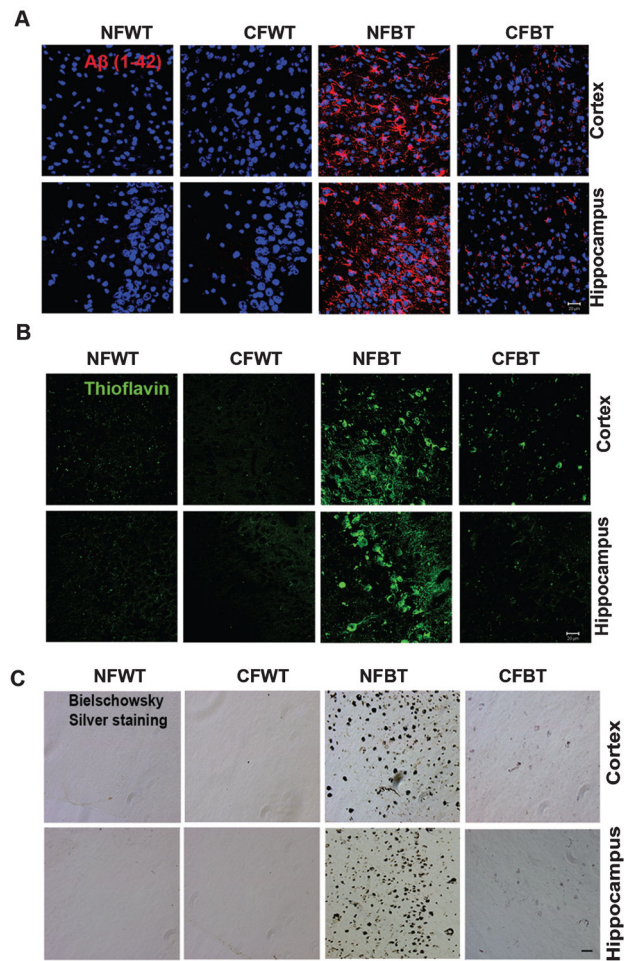
Fig. 5.
Amyloid accumulation is reduced in curcumin-treated p25Tg mice. A) Representative immunofluorescence images from the cortex (layer 2/3) (top panels) and hippocampus (CA3 region) (bottom panels) of the brain sections from 18-week-old wild type mice with normal feed (NFWT), wild type mice with curcumin feed (CFWT), 12-week induced (18-week-old) p25Tg mice with normal feed (NFBT), and p25Tg mice with curcumin feed (CFBT) ($n = 3$) using anti-Aβ_{1-42} antibody (red) and DAPI (blue). Thioflavin-S staining images (B) and Bielschowsky silver staining images (C) from the brain sections of the mice groups same as in (A). Scale bars represent 20 μm.
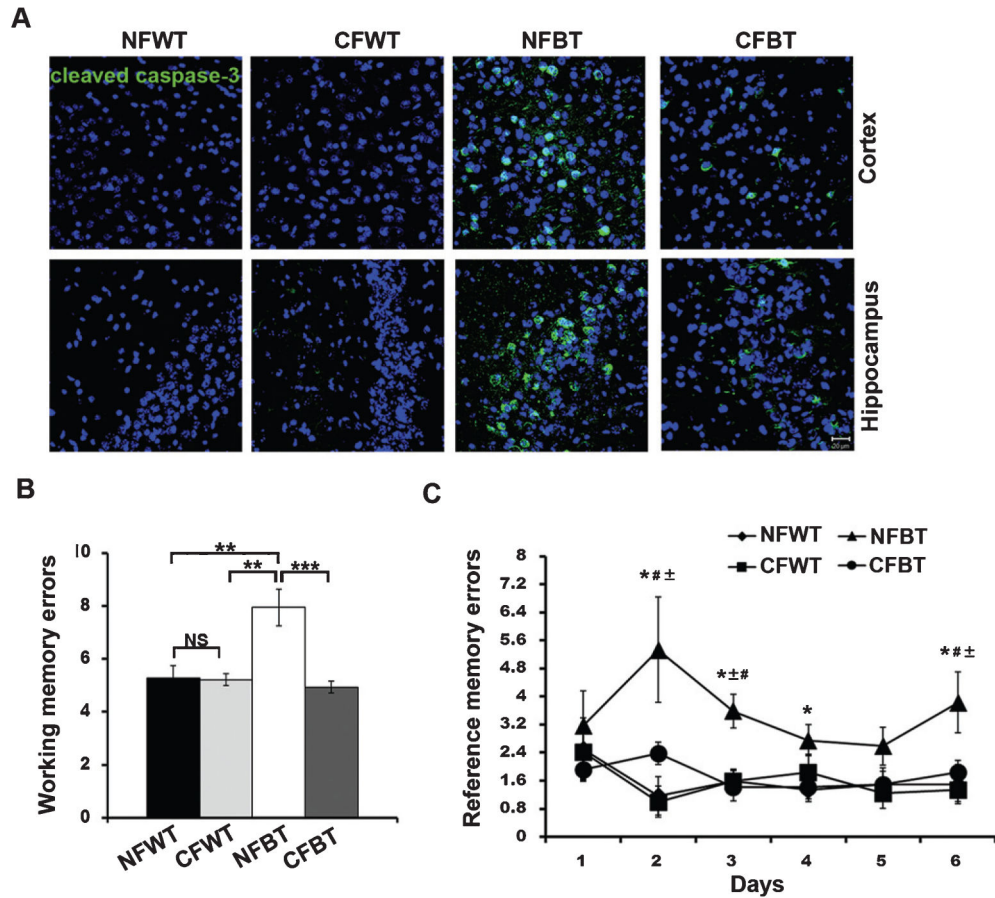
Fig. 6.
Curcumin reduces neuronal apoptosis and ameliorates cognitive deficits in p25Tg mice. A) Brain sections from the cortex (layer 2/3) (top panels) and hippocampus (CA3 region) (bottom panels) of 18-week-old wild type mice with normal feed (NFWT), wild type mice with curcumin feed (CFWT), 12-week induced (18-week-old) p25Tg mice with normal feed (NFBT), and p25Tg mice with curcumin feed (CFBT) ($n = 3$) were immunostained with anti-cleaved caspase-3 antibody (green) and DAPI (blue). Scale bars represent 20 μm. B, C) Eight-arm radial maze performance was examined for 12-week induced NFBT ($n = 5$), CFBT ($n = 6$), NFWT ($n = 5$), and CFWT ($n = 6$) mice. B) Bar graph represents the average number of working memory errors (average of 10 sessions) (**$p < 0.01$) (one-way ANOVA followed by *post-hoc* Tukey's test) and (C) line graph represents the average number of reference memory errors (average of sessions per day (10 sessions in 6 days)) (*$p < 0.05$ compared to NFWT mice, #$p < 0.05$ compared to CFWT mice and ±$p < 0.05$ compared to CFBT mice) (repeated measures ANOVA followed by *post hoc* Tukey's test). Error bars indicate ± s.e.m.